Load Reduction in Lead-Lag Dampers by Speed-Scheduled Aperture and Modulated Control of a By-Pass Valve*

C.L. Bottasso[†], **S. Cacciola**[‡], **A. Croce**[§], **L. Dozio**[¶]
Politecnico di Milano
Milano, Italy

Abstract
Existing hydraulic dampers are passive devices, and their damping characteristics cannot be adapted to the varying damping needs of each different flight condition of a rotorcraft. Therefore, dampers and their interfaces to the rotor system are constantly subjected to large damping forces, which contribute to their damage and wear. In this work we consider the possible use of a by-pass valve as a means to reduce loads while still providing the required amount of damping for safe flight. Two different policies for the use of the by-pass are considered: in the first and simplest of the two, the valve is opened of a constant amount which varies only as a function of the vehicle flight speed, while in the second the valve aperture is modulated as a function of blade azimuth using a higher harmonic feedback law. The investigation on the load-reduction capabilities of the by-pass augmented damper is conducted by using validated mathematical models of the A109E Power helicopter and of its damper. It is found that both policies are capable of delivering the required level of damping at substantially reduced loads, which for the speed-scheduled aperture drop at values that range between 30-60%, depending on the flight condition, of the loads generated by the standard passive device, and for the higher harmonic modulated law at values around 20-25%.

INTRODUCTION AND MOTIVATION

There is a basic dilemma in the design of lead-lag dampers for helicopter rotors: high damping levels are necessary for the stability of the system in a very small range of the flight envelope, that typically includes the conditions of vehicle on the ground, in slope landings or during high-g maneuvers; on the other hand, much lower damping levels would be appropriate for all other flight regimes. Unfortunately, current lead-lag dampers are *passive* devices. As such, they are designed so as to provide the necessary damping in the damping-crucial portions of the flight envelope, but are unable to change their behavior according to the flight regime. This implies that they are invariably subjected to large damping forces, even in those flight conditions where high damping is not necessary. Such loading contributes to the rapid wear and aging of the dampers and of their interfaces with the rotor system, with resulting significant operating and maintenance costs. Notice that this problem is common to all current design solutions for rotor dampers, including hydraulic, elastomeric and fluid-elastic technologies.

In this paper, we address this problem by considering a hydraulic damper equipped with a by-pass valve. The opening of the valve can be used to increase the flow of fluid between the two hydraulic chambers of the damper, affecting both the internal forces and the resulting damping of the system. Goal of the present investigation is to evaluate the effectiveness of the by-pass valve as a load-reduction device, trying to answer the following two questions:

1. Since in most flight conditions the system has more damping than necessary, can we significantly reduce the loads if we allow for a decrease in the damping to lower but still safe values?

2. If so, can load reductions be achieved by a straightforward scheduled aperture, i.e. the simple opening of the by-pass valve as a function of the flight condition (e.g., in terms of the flight speed), or do we need more sophisticated modulating control laws that vary the valve opening as a function of the blade motion?

The paper does not address the related interesting problem of using modulations in the valve aperture to selectively provide damping in the lag mode. This additional use of the by-pass valve, although possible in

*Presented at the American Helicopter Society 66th Annual Forum and Technology Display, May 11–13, 2010, Phoenix Convention Center, Phoenix, AZ, USA.

[†]Professor, e-mail: carlo.bottasso@polimi.it.
[‡]Ph.D. candidate.
[§]Assistant Professor.
[¶]Assistant Professor.

theory and potentially useful for certain applications, would appear not to be required for the system considered here, as it will seen in the results section.

Clearly, the idea of using a by-pass valve in hydraulic dampers is not new. For example, a mechanical device for the selective damping of the lag frequency is described in Ref. [1], while the use of a by-pass valve was investigated in Ref. [2] with regard to the reduction of vibratory hub loads. Reference [3] deals with the modeling and analysis of semi-active hydraulic dampers operating in the periodic environments typical of rotary wing vehicles, while Ref. [4] describes the integration of a hydraulic lead-lag damper equipped with a by-pass valve with a helicopter rotor simulation code.

The recent literature explores also alternative non-hydraulic technologies for realizing semi-active dampers. For example, in Ref. [5] ground resonance conditions are stabilized by using feedback control and semi-active magnetorheological dampers, while Ref. [6] proposes the use of a magnetorheological valve in the inner chamber of an elastomeric damper; yet another solution is investigated in Ref. [7], where the authors consider semi-active lead-lag dampers based on the use of Coulomb friction, whereby damping is modified through the modulation of the normal force component at the frictional interface in the device.

While it appears to be possible to realize semi-active dampers using a variety of technological solutions, the present paper focuses on the semi-active hydraulic one. In fact, a by-pass valve is a relatively straightforward addition to the existing and by now very well proven hydraulic damping technology. Although rather simple, such modification allows for a completely passive device to be turned into a semi-active one without a major redesign or a radical change of technology, which would invariably raise a number of issues on the practical applicability in the field of a completely new device. The fact that hydraulic dampers still equip most existing helicopters, and especially the heaviest ones, provides for an important motivation for studying the feasibility and assessing the possible payoffs of such a solution.

APPROACH AND METHODS

The present study was conducted with reference to the A109E Power helicopter. At first, a mathematical model of its damper was developed, including a by-pass valve. The characteristic curves of the modified damper were then used in the definition of a mathematical model of the helicopter rotor. Next, the vehicle was trimmed at a number of relevant flight conditions, and the performance of the semi-active damper was evaluated for different scheduled aperture and modulating control laws, by assessing the resulting forces and damping factors.

Mathematical Model of the Damper

In this work, controllable damping is achieved by adding a by-pass valve to a conventional hydraulic mono-tube damper configuration. The by-pass valve allows a path for the fluid to and from the two hydraulic chambers, thereby affecting the pressure resultant on the piston. The design considered here features an electro-mechanical actuator providing the tunable force that moves the valve spool, which in turn modifies the outflow area; a pre-loaded spring returns the spool in the shut position in case of loss of power, reverting the system to a standard passive damper.

The physics-based mathematical model of the hydraulic damper includes the pressure dynamics equations in the two chambers, and the pressure/flow equations through the orifice, the pressure relief valves and the actuated by-pass valve. This set of equations is coupled to the equations of motion of the piston and valve poppets, which include friction and impact effects. The resulting model is expressed in terms of a coupled set of non-linear ordinary differential equations, reported in the appendix, that yield the response of the damper force given the motion as input.

The mathematical model was tuned by identifying the values of the orifice and relief valve discharge coefficients and of the relief valve pre-load so as to match experimental load-speed curves, provided by the damper manufacturer. The experimental data was obtained by subjecting the damper to sinusoidal strokes of given frequency and amplitude; similarly, the mathematical damper model was subjected to the same inputs. For each frequency and amplitude, a load-speed characteristic curve of the damper was traced by plotting the resulting peak load and peak speed. For a given frequency, Fig. 1 reports the experimentally measured and numerically computed (solid line) characteristic curves, showing a good correlation of the latter with the former. For low speeds the relief valves are closed and the characteristic curve has an approximately parabolic behavior, while for higher speeds the valves are open and the curve is almost linear. On the other hand, the progressive opening of the relief valves determine the location and shape of the curve “knee” in the transition region.

Figure 2 illustrates the effects on the characteristic curve for a constant opening of the by-pass valve $\Delta_{\mathrm{byp}} = A_{\mathrm{byp}}/A_{\mathrm{or}}$, where A_{byp} is the by-pass opening area and A_{or} the area of the equivalent orifice (see the appendix). It appears that the main effect of the by-pass is a delay with respect to the stroke speed of the opening of the pressure relief valves, which in turn implies that, for the same speed, the damping forces are rapidly reduced with increasing openings of the valve.

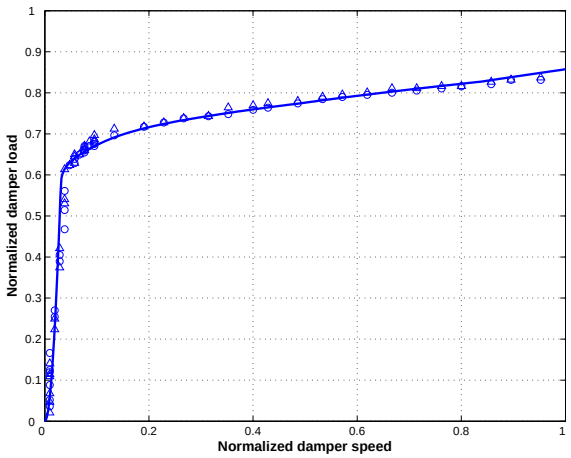

Figure 1: Load-speed characteristic damper curve. Mathematical model: solid line; experimental data: triangle (compression) and circle (expansion). Values are scaled to protect proprietary data.

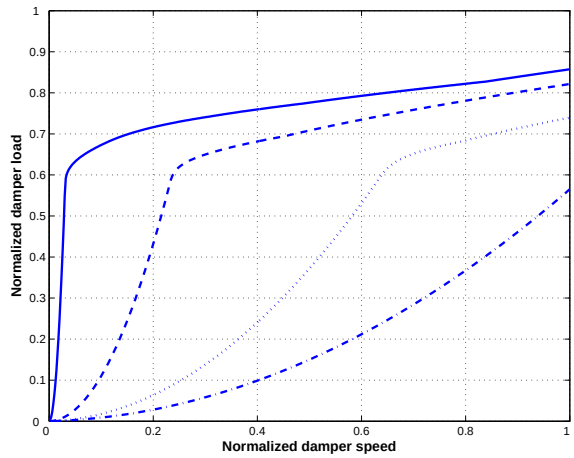

Figure 2: Effects on the characteristic curve of a constant opening of the by-pass valve. $\Delta_{\text{byp}} = 0$ (standard damper): solid line; $\Delta_{\text{byp}} = 10$: dashed line; $\Delta_{\text{byp}} = 30$: dotted line; $\Delta_{\text{byp}} = 50$: dash-dotted line.

Model of the A109E Power Helicopter

The helicopter model is based on a detailed multibody model of the main rotor, based on the formulation of Ref. [8], coupled to a rigid body model of the fuselage for the trimming in free flight of the vehicle. The rotor model, symbolically depicted in Fig. 3, includes elastic blades and a complete kinematically accurate representation of the control linkages, including rotating and non-rotating swash-plate with scissors, pitch-links and lead-lag dampers.

Since the characteristic time scales of the aeroelastic rotor model are much longer than the ones of the hydraulic damper, which is governed by very stiff equations with discontinuous coefficients, a direct strong coupling of the two models was avoided in favor of a simpler one-way approximate coupling. To this end, the mechanical characteristics of the damper were obtained by integrating the damper governing equations for assigned sinusoidal stroking motions of given amplitude and frequency; the resulting force-speed characteristic curves were stored in table-look-up form and used at run time during the multibody transient simulations.

The coupled model was validated with the help of test flight data provided by the helicopter manufacturer, which included trim control values and associated damper stroke time histories, achieving a good matching between simulations and experimental data. For example, Table 1 reports the percent error of the maximum damper load computed using the mathematical model and the maximum damper load measured in flight, for values of the flight speed between 0.8 and 1.0 V_{NE} (where V_{NE} is the never-exceed speed of the helicopter), since these are the flight conditions that contribute the most to the damage of the damper.

Flight speed	Percent error
0.80 V_{NE}	-5.4%
0.90 V_{NE}	-1.9%
0.95 V_{NE}	0.1%
1.00 V_{NE}	1.0%

Table 1: Percent error of simulated maximum damper loads with respect to flight test measurements, as a function of flight speed.

The wide separation of aeroelastic and hydraulic time scales and the good correlation of the results with experimental observations, justify the present simplified approach, although stronger coupling strategies of the aeroelastic and hydraulic models could be developed following the indications of Refs. [4, 9].

Control Laws

The load-reducing control architecture considered in this work is depicted in Fig. 4.

The internal loop consists of a speed-scheduled aperture of the by-pass: the valve opens of a given amount for each given flight speed, and no modulation of the opening is performed as a function of the blade/damper azimuth and/or response. This solution has the characteristic of maximum possible simplicity within this technology and hence the maximum chance

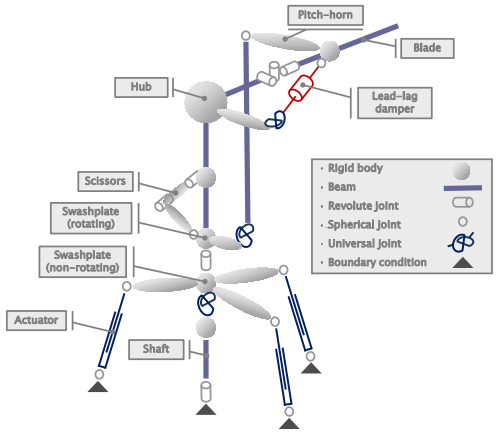

Figure 3: Detailed multibody model of the rotor system, including control linkages and damper (one single blade shown for clarity).

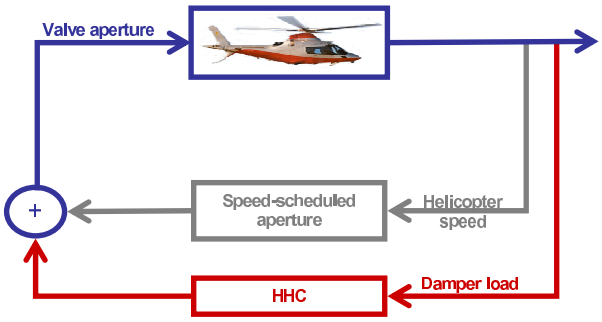

Figure 4: Load-reducing control architecture.

of actual applicability in the field. On the other hand, it implements a static modification of the damper that does not account for the response of the coupled rotor-damper system.

The (optional) external control loop is a higher harmonic controller (HHC) (cf. Refs. [10, 11, 12] and references therein) that, on top of the speed-scheduled constant valve aperture, modulates in time an additional valve opening with the goal of further reducing the load harmonic amplitudes. This requires the implementation of a feedback controller on-board the vehicle using stroke-measuring sensors, which implies an additional level of complexity with respect to the simple scheduled-aperture solution, but has the potential for further load reduction margins, as shown later on. If such a solution turns out to be necessary/desirable, so that the device is equipped with the necessary computing hardware and sensors, one could clearly think of adding a third control loop for providing selective damping in the lag mode, in case a damping increase is deemed necessary for the stability of the system. However, it will be shown later on in the results section that, as far as the present investigation is concerned, selective lag damping control appears not to be necessary, and only the two loops of Fig. 4 will be considered here.

The HHC loop is synthesized on the basis of a linear input-output model in the frequency domain, which writes

$$z = z_0 + \boldsymbol{\Theta}\boldsymbol{\beta}, \tag{1}$$

where z is the output vector of damper load harmonics, $\boldsymbol{\beta}$ the input vector of by-pass valve opening harmonics, z_0 the baseline damper load harmonics in the absence of HHC control inputs, and $\boldsymbol{\Theta} = \partial z/\partial\boldsymbol{\beta}$ the matrix of output/input sensitivities. The model unknowns z_0 and $\boldsymbol{\Theta}$ were identified by exciting the system with known inputs at the harmonics of interest, recording and demodulating the response, and estimating the coefficients using least squares (see Ref. [10]).

The optimal input harmonics $\boldsymbol{\beta}_{\mathrm{HHC}}$ are computed by minimizing the quadratic cost function

$$J = \frac{1}{2}(z^T \boldsymbol{Q} z + \boldsymbol{\beta}^T \boldsymbol{R}\boldsymbol{\beta}), \tag{2}$$

where $\boldsymbol{Q}$ and $\boldsymbol{R}$ are weight matrices, which results in the feedback law

$$\boldsymbol{\beta}_{\mathrm{HHC}} = -(\boldsymbol{\Theta}^T \boldsymbol{Q}\boldsymbol{\Theta} + \boldsymbol{R})^{-1}\boldsymbol{\Theta}^T \boldsymbol{Q} z_0. \tag{3}$$

These by-pass valve harmonics are then modulated in terms of the rotor azimuth and added to the speed-scheduled opening to give the total by-pass aperture at each azimuthal blade location.

Estimation of Damping

The estimation of damping in the lag response of the system was performed using Prony's method (cf. Refs. [13, 14, 15]), modified as described in Ref. [16] so as to account for the periodic nature of the problem. In fact, when using Prony's method the system is assumed to be represented by a linear time invariant (LTI) system around an equilibrium condition, and the response recorded following a suitable excitation is used for identifying a discrete time auto-regressive (AR) model (Ref. [17]). Finally, computing the discrete poles of the system and transforming to continuous time using Tustin transformation, gives the damping factors of the modes of interest.

This standard formulation does not account for the fact that the dynamics of the helicopter in the neighborhood of a trim equilibrium condition can be more appropriately modeled as a linear time periodic (LTP) system, rather than in terms of an LTI, as discussed for example in Ref. [18]. Hence, the approach used here is to start from an LTP, which more faithfully represents the physics of the problem, and then approximate it in order to obtain an equivalent LTI. Since the obtainment of the

equivalent LTI requires the introduction of an additional exogenous periodic input into the system, as shown below, a discrete time auto-regressive model with exogenous input (ARX) is used in this formulation for the identification of the input-output relationship. Damping factors are then computed as in the classical case by computing the discrete poles and transforming to continuous time.

The helicopter closed-loop dynamics can be written in state space LTP form as

$$\dot{\boldsymbol{x}} = \boldsymbol{A}(\psi)\boldsymbol{x} + \boldsymbol{B}(\psi)u, \tag{4}$$

where ψ is the rotor azimuth, $\boldsymbol{x}$ the state vector, $\boldsymbol{A}(\psi)$ the closed-loop periodic system matrix (i.e. accounting for the loop closure performed by the flight control system on the rotor collective, longitudinal and lateral pitch control inputs), while u is an equivalent exogenous constant scalar input which, together with its associated periodic matrix $\boldsymbol{B}(\psi)$, models the periodic excitations generated by the aerodynamic and gravitational loads.

Using the Fourier reformulation (see Ref. [19]), the periodic matrices $\boldsymbol{A}(\psi)$ and $\boldsymbol{B}(\psi)$ can be rewritten as

$$\boldsymbol{A}(\psi) = \boldsymbol{A}_0 + \sum_k \left(\boldsymbol{A}_{sk}\sin(k\psi) + \boldsymbol{A}_{ck}\cos(k\psi)\right), \tag{5a}$$

$$\boldsymbol{B}(\psi) = \boldsymbol{B}_0 + \sum_k \left(\boldsymbol{B}_{sk}\sin(k\psi) + \boldsymbol{B}_{ck}\cos(k\psi)\right). \tag{5b}$$

An LTI approximation to the LTP (4) is obtained by arresting the Fourier expansion of the state matrix $\boldsymbol{A}(\psi)$ at the constant term, i.e. using $\boldsymbol{A}(\psi) \approx \boldsymbol{A}_0$, and transferring the periodicity of the $\boldsymbol{B}(\psi)$ matrix to its associated input term u, i.e. setting $\boldsymbol{B}(\psi)u = \boldsymbol{U}\boldsymbol{b}(\psi)$ where $\boldsymbol{U}$ is a constant matrix and $\boldsymbol{b}(\psi)$ an exogenous periodic input. This yields the following LTI in state space form

$$\dot{\boldsymbol{x}} = \boldsymbol{A}_0\boldsymbol{x} + \boldsymbol{U}\boldsymbol{b}(\psi). \tag{6}$$

Introducing the outputs, which are in this case represented by the damper stroke, an ARX input-output model can be obtained by transforming Eq. (6) into discrete time and by eliminating the states on a sequence of steps (see Ref. [17]), which leads to the following regression

$$\begin{aligned} y(iT) = \\ a_1 y\big((i-1)T\big) + a_2 y\big((i-2)T\big) + \ldots + a_n y\big((i-n)T\big) + \\ u_1 b\big((i-1)T\big) + u_2 b\big((i-2)T\big) + \ldots + u_m b\big((i-m)T\big) + \\ \eta(iT), \end{aligned} \tag{7}$$

$i = \max(m,n)+1, N$, where T is the sampling step, $\{a_1,\ldots,a_n\}$ and $\{u_1,\ldots u_m\}$ are respectively the n and m unknown auto-regressive and exogenous parameters, and η the zero mean uncorrelated measurement error with constant variance.

The estimation of the unknown ARX parameters proceeds as follows. First, the system is subjected to a doublet (i.e. a two-sided pulse) torque input at the lag hinge, starting from each trim condition of interest, and the ensuing free damper stroke response $y(iT)$ is recorded over N time steps. Next, the exogenous input $b(iT)$ is generated using all harmonics of interest; notice that the input amplitudes are arbitrary, since the associated coefficients u_j are unknown, and therefore they can all be set to the value of one. Finally, the equation error method is used for estimating the parameters from the given input-output sequence (cf. Ref. [17]). Once the parameters are known, the damping factors are readily obtained.

Figure 5 illustrates the quality of the models that were obtained with this approach. Figure 5(a) gives a time-domain comparison, reporting the time history of the recorded damper stroke (solid line) and the one generated using the identified model (dashed line); Fig. 5(b) gives a frequency-domain comparison, reporting the recorded (solid line) and simulated (dashed line) harmonic amplitudes which show the peaks at the 1, 2 and 3 per rev, as well as the lag mode at 1.7 Hz. Both in the time and the frequency domains, the identified model displays and excellent match to the recorded datum, supporting the hypothesis that $\boldsymbol{A}(\psi) \approx \boldsymbol{A}_0$.

RESULTS

As previously stated, in order to judge on the suitability of a by-pass-augmented damper, it is crucial to assess its load reduction capabilities, in the light of a possibly reduced damping in the lag mode, considering a not-to-exceed lower safety limit. For this investigation, the helicopter manufacturer indicated as lower margin the 30% of the damping factor provided by the original passive damper in the same flight condition. This value was based on an independent investigation that considered air resonance and other criteria for safe flight and appropriate handling qualities.

Based on these indications, the best scheduling of the by-pass aperture was determined by minimizing the peak loads without exceeding the allowed damping loss at each flight condition of interest. The results of this investigation, conducted by progressively increasing the by-pass aperture until the lower damping limit is encountered, are shown in Fig. 6. Figure 6(a) shows, for different flight speeds, the damping factor as a functions of the valve aperture Δ_{byp}. Notice that a value of $\Delta_{\text{byp}} = 100$ corresponds to about one half of the characteristic area $\pi d_{vi}^2/4$ of the pressure relief valves (see Eq. (10) in the appendix). A thick solid line shows the lower damping limits according to the 30% criterion. Similarly, Fig. 6(b) shows the corresponding damper loads (normalized, so as to protect proprietary information). The percent damper load reductions which are achieved at the lower damping margin are summa-

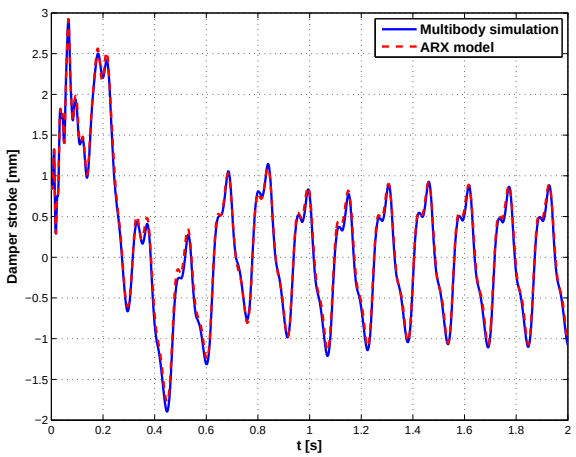

(a) Time-domain comparison

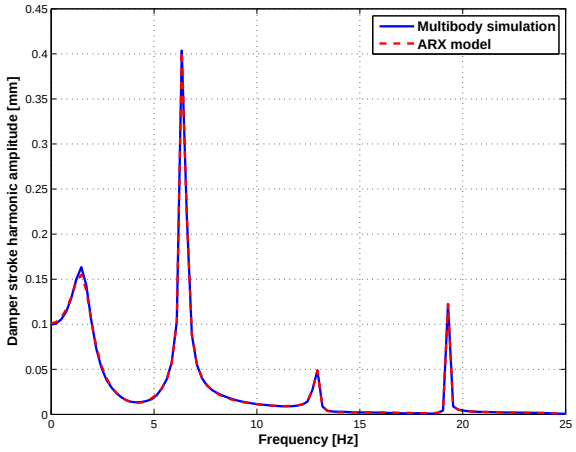

(b) Frequency-domain comparison

Figure 5: Damper stroke response after perturbation, in the time (a) and frequency (b) domains. Plant, i.e. multibody vehicle model: solid line; identified ARX model: dashed line.

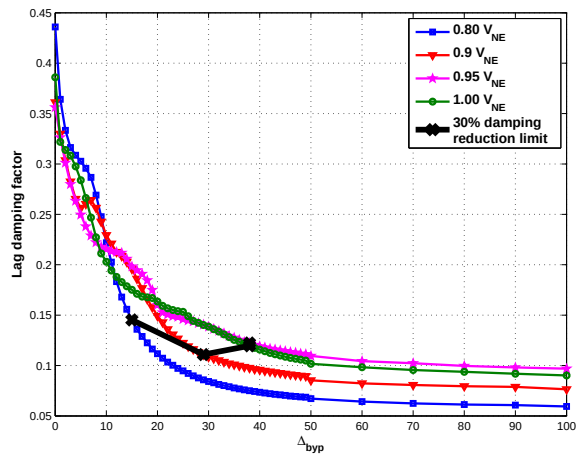

(a) Damping factor

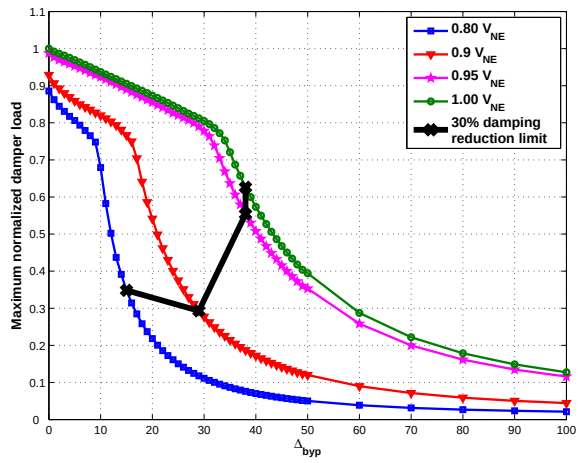

(b) Maximum load

Figure 6: Damping factors (top) and maximum damper loads (bottom) as functions of by-pass valve opening, for varying flight speeds.

rized in Table 2, together with their associated valve apertures.

The results of Fig. 6 allow for some interesting observations. First, reducing the damping to the 30% of the one provided by the baseline passive damper, comes accompanied by substantial reductions in the damper loads at all flight speeds thanks to the quick drop of the loads with increasing valve apertures. Second, the necessary by-pass valve apertures are large, but not so large to completely eliminate the damping effects provided by the hydraulic damper. In other words, the lower damping constraints would not be satisfied by completely eliminating the damper, as it can be seen by comparing in Fig. 6(a) the location of the thick solid line marking the damping constraints with the asymptotic damping factor values at the higher by-pass apertures, which correspond to the inherent (aerodynamical) damping of the rotor.

Next, we investigated the effects of the introduction of the HHC loop in the by-pass opening policy. Figure 7 reports the damper load (top) and the associated by-pass aperture (bottom) as functions of the blade azimuth for two rotor revolutions, in steady level fight at 1.0 V_{NE}. Note the significant load reduction achieved by the simple speed-scheduled aperture with respect to the passive case, but also the additional ability of the HHC loop in further lowering the load peaks. Examining Fig. 7(b) it appears that HHC requires a maximum aperture of the by-pass valve close to the value of 68, which is substantially larger than in the speed-scheduled case (38). Notice that a constant valve aperture of this magnitude would almost completely eliminate the damping effects provided by the hydraulic damper, as shown in Fig. 6(a).

Further insight on the functioning of the adaptive damper can be obtained by examining Fig. 8, which

Flight speed	Δ_{byp}	Load reduction
0.80 V_{NE}	15	-60.7%
0.90 V_{NE}	29	-68.4%
0.95 V_{NE}	38	-43.9%
1.00 V_{NE}	38	-37.4%

Table 2: By-pass apertures and corresponding load reductions for varying flight speed, for damping factors satisfying the 30% reduction margin.

gives the trajectories of the damper response in the load-speed plane. Figure 8(a) corresponds to the case of a small maximum allowed by-pass aperture; the opening of the valve is not large enough to prevent the activation of the pressure relief valves (notice the trajectories passing the curve knees) and load reduction is therefore not significant. On the contrary, Fig. 8(b) corresponds to the case of a larger maximum allowed aperture, such that the damper can always operate in the parabolic region of the load-speed characteristic curves, with reduced peak loads.

The results of the investigation on the effectiveness of the HHC-augmented solution are summarized in Fig. 9 and Table 3. Figure 9(a) reports the damping factor of the lag mode as a function of the vehicle flight speed, for the standard passive damper, the scheduled-aperture solution and the HHC-modulated one. For both semi-active damper solutions, the reduction in damping with respect to the passive case never exceeds the assigned safe lower limit. This seems to indicate that in all cases the device retains enough damping ability to meet the stability goals, even when the by-pass valve is opened to reduce the loads. This has potentially interesting implications, since it indicates that an additional control loop for the increase of damping in the lag mode, as previously hypothesized, is probably not necessary.

Figure 9(b) reports the maximum damper load as a function of the vehicle flight speed, for the standard passive damper, the scheduled-aperture solution and the HHC-modulated one. It appears that both semi-active damper solutions are capable of very significantly reducing the peak loads. Furthermore, the results show that the active-modulation HHC solution is indeed capable of important further reductions of the peak loads with respect to the simple scheduled-aperture one (cfr. Table 3). However, since the reduction obtainable with the simpler scheduled-aperture is

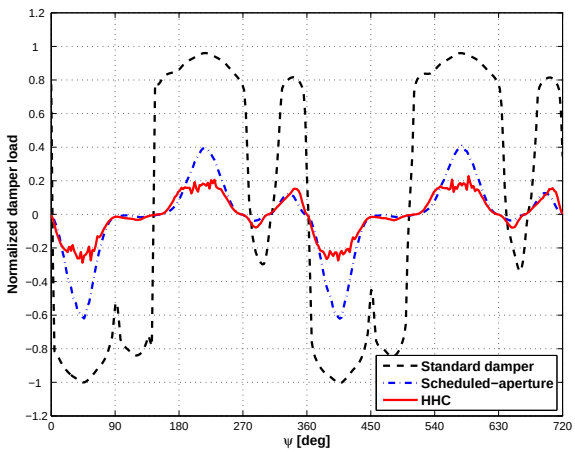

(a) Damper load

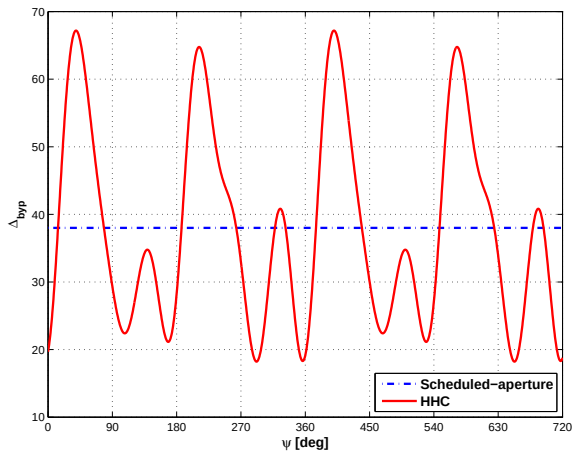

(b) Δ_{byp}

Figure 7: Damper load (top) and by-pass aperture (bottom) vs. blade azimuth for two rotor revolutions, at 1.0 V_{NE}. Standard passive damper: dashed line; speed-scheduled aperture: dash-dotted line; speed-scheduled aperture and HHC: solid line.

already significant, the decision on whether to adopt such an active-modulation solution or not must in the end consider all trade-offs between increased complexity (with its impacts on cost and reliability) and improved performance, something that is outside of the scopes of the present investigation and is better left to the damper manufacturer.

CONCLUSIONS

In this work, we have developed and validated a mathematical model of a helicopter equipped with a hydraulic lead-lag damper, and we have used it to investigate the possible reductions in the damper loads that can be achieved by the use of a by-pass valve. The study was conducted by assuming that in all flight conditions the

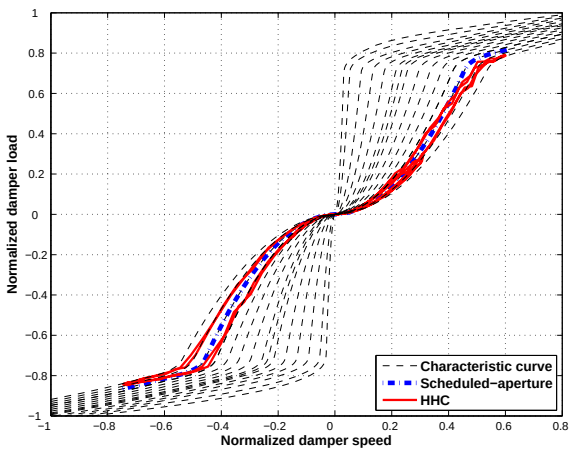

(a) Maximum by-pass aperture: $\Delta_{\text{byp}} = 25$

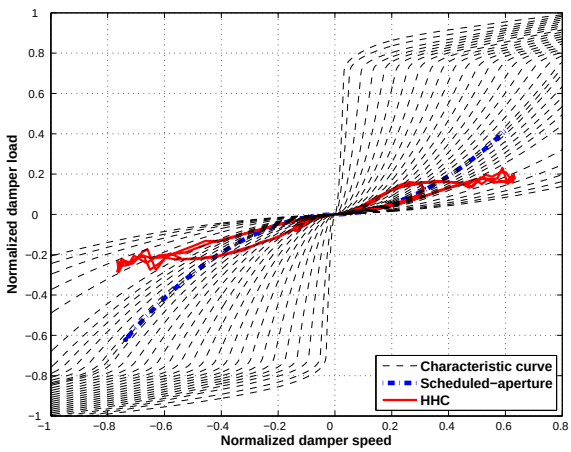

(b) Maximum by-pass aperture: $\Delta_{\text{byp}} = 68$

Figure 8: Trajectories of the damper response in the load-speed plane, for small (top) and large (bottom) maximum by-pass apertures. Speed-scheduled aperture: dash-dotted line; speed-scheduled aperture and HHC: solid line.

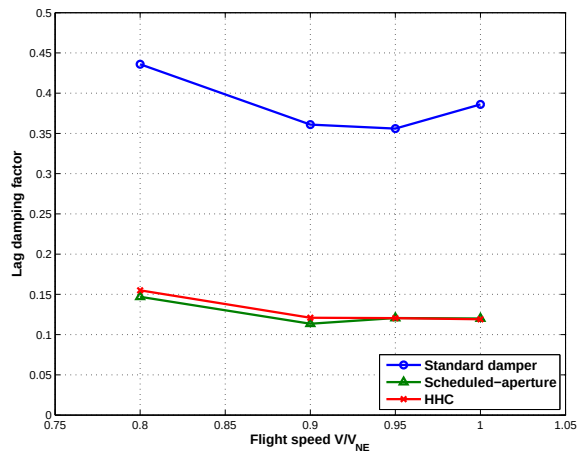

(a) Damping factor

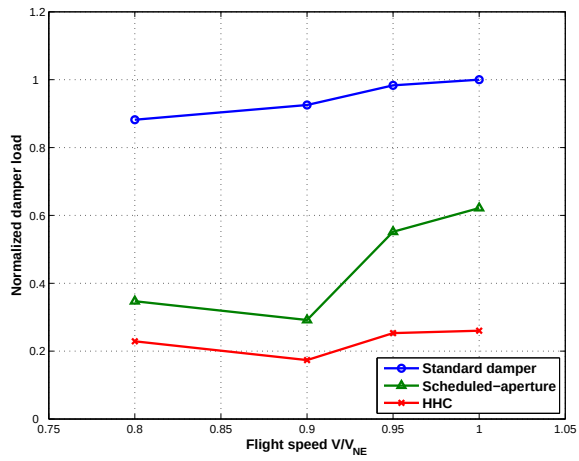

(b) Maximum load

Figure 9: Damping factors (top) and maximum damper loads (bottom) as functions of flight speed, for the standard passive damper, and for the speed-scheduled aperture and HHC-augmented solutions.

damping factor can be lowered to a safe fraction, 30% in this case, of the damping provided by the standard passive version of the device. Measurement of damping in flight was performed with a new modified version of Prony's method, that explicitly accounts for the periodic nature of the rotorcraft mathematical model. We have investigated two possible uses of the by-pass valve: a simple constant opening that varies only with the vehicle flight speed, and a more sophisticated modulation of the valve position based on a HHC feedback loop.

Based on the results of the present study, the following conclusions can be drawn:

- Even the straightforward speed-scheduled aperture of the by-pass valve is capable of significant reductions in the damper loads, which were here found to be lowered to approximatively the 30-60% of the ones of the passive device for the level forward flight conditions that most contribute to the accumulation of damage in the damper.
- The satisfaction of the 30% safe damping margin is achieved with openings of the valve in the range of about 15-40 times the area of the equivalent orifice. With these openings, the device still contributes some significant damping in addition to the intrinsic aerodynamic damping of the rotor.
- The HHC modulation of the by-pass valve on top of the speed-scheduled aperture allows for an even greater reduction of the loads, which drop to values in the range of 20-25% of the ones of the passive device, while still satisfying the lower damping margin constraint.
- The HHC by-pass modulation requires maximum

Flight speed	Load reduction wrt passive damper	Load reduction wrt scheduled aperture
0.80 V_{NE}	-74.0%	-34.0%
0.90 V_{NE}	-81.2%	-40.6%
0.95 V_{NE}	-74.3%	-54.1%
1.00 V_{NE}	-74.0%	-58.1%

Table 3: Load reductions of the HHC-augmented solution for varying flight speed, with respect to the standard passive damper and the speed-scheduled aperture control policy.

valve openings of about 70 times the area of the equivalent orifice, values that, if kept constant instead of being modulated by the HHC feedback law as a function of blade azimuth, would practically eliminate all damping provided by the device to the rotor system.

- It appears that the semi-active by-pass system, both in the case of the simple speed-scheduled aperture and of the HHC modulation, retains the ability to provide the required level of damping to the rotor system; in this sense, it appears that additional control loops aimed at selectively increasing the damping of the lag mode are not necessary.

Clearly, although the above results seem promising, the present study provides only preliminary indications on the potential applicability of this technology to a real rotor system and there are several topics that would merit further investigation:

- In the area of aeromechanic analysis, one should probably perform a more detailed investigation of the minimum damping requirements by directly studying air-resonance, high-g turns and all other damping critical flight conditions; although the 30% damping lower constraint was provided by the helicopter manufacturer on the basis of an independent study accounting for such conditions, it is possible that further margins for improvement might be achieved by the direct simulation of all flight conditions of interest with the coupled semi-active damper/vehicle models that were developed here.
- It would be interesting to be able to translate the load reductions computed here in extended life of the damper and of its interfaces to the rotor system, so as to be able to quantify possible savings.
- The development of an experimental facility comprising a modified hydraulic damper with by-pass valve and a damper test bench would allow for the verification of several key aspects of this technology, and provide data for the validation of the mathematical models. The semi-active damper should also be tested in rotation, to simulate the centrifugal forces experienced by the device on the rotor.
- The trade-offs existing between improved performance achievable by the HHC (or other control law) modulation and the increased system complexity to support such sophisticated by-pass activation, would need to be fully understood.

ACKNOWLEDGEMENTS

The research described in this document is funded by MECAER Meccanica Aeronautica S.p.A. through a grant of the Italian Ministry of Defense. The contribution of D. Devecchi of the Politecnico di Milano and of G. Clemente and L. Miroballi of MECAER is gratefully recognized. The authors acknowledge the contribution of AgustaWestland in making available modeling and validation data of the A109E Power helicopter, and for valuable feedback.

APPENDIX A: MATHEMATICAL MODEL OF THE DAMPER

Hydraulic damper models, as those discussed in Refs. [20, 21], are invariably associated with significantly non-linear response characteristics (see Refs. [22, 23]), which are primarily due to turbulent flow, fluid compressibility, friction and pressure relief. The modeling of these effects leads to a set of coupled non-linear differential equations that depend on several parameters; clearly, for these models to yield faithful predictions, the values of their parameters should be known with reasonable accuracy or should be identified from experimental data, as done in the course of the present work.

The baseline model used here of hydraulic damper with pressure relief valves involves two hydraulic chambers separated by a movable piston, as symbolically depicted in Fig. 10.

The pressure dynamics in the ith chamber, $i = 1,2$, can be written as

$$\dot{p}_i = \frac{\beta}{V_i}\Big(\sum_j q_j - (-1)^i A \dot{x}_\mathrm{p}\Big), \tag{8}$$

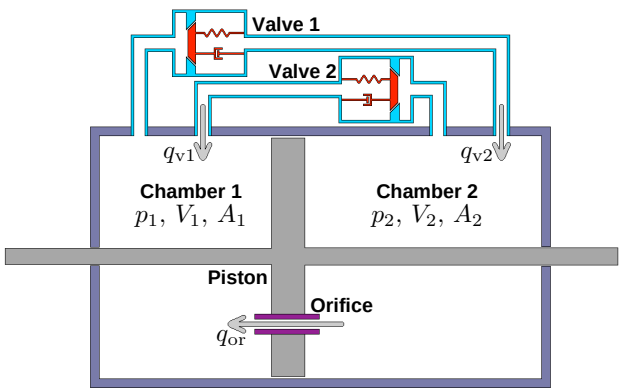

Figure 10: Conceptual sketch of the conventional damper. In the real damper, the pressure relief valves and orifices are located on the piston.

where p_i is the pressure, V_i the chamber volume with initial value V_{0i}, A is the area of the piston, x_p its displacement, positive if it reduces the volume of chamber 1, and β is the oil bulk modulus. Oil volumetric flow rates are noted q_j, positive if incoming and negative if outgoing, and include the flow through the pressure relief valves, the hydraulic orifices and the by-pass valve.

The flow through the ith valve, $i = 1,2$, is

$$q_{vi} = c_d^v A_{ovi}(x_{ri})\sqrt{\frac{2}{\rho}|p_2 - p_1|}\,\mathrm{sign}(p_2 - p_1), \tag{9}$$

where ρ is the oil density, x_{ri} is the relative displacement between valve and piston, c_d^v is the valve outflow coefficient, and A_{ovi} the effective outflow area, which in turn depends on the valve opening as

$$A_{ovi}(x_{ri}) = \pi d_{vi} x_{ri} \sin\theta_i, \tag{10}$$

where d_{vi} is the diameter of the passage section and θ_i is the outflow angle. The valve outflow coefficient is expressed as a function of the valve opening (see Refs. [24, 25] for details) as

$$c_d^v = \bar{c}_d^v \frac{\gamma x_{ri}}{1 + \gamma x_{ri}}, \tag{11}$$

where $\bar{c}_d^v$ is the asymptotic value of the outflow coefficient for $x_{ri} \to \infty$, and γ is a tuning parameter.

The ith valve dynamic equation, $i = 1,2$, writes

$$\ddot{x}_{ri} = \frac{1}{m_{vi}}\big(-c_{vi}\dot{x}_{ri} - k_{vi}x_{ri} + (p_2 - p_1)A_{vi} - (-1)^i F_{pri} - m_{vi}\ddot{x}_p\big), \tag{12}$$

where F_{pr} is the force pre-load. The contact-impact conditions between valve poppet and piston are modeled using Newton's method, which gives rise to the following initial conditions on the poppet position and speed immediately after a contact event

$$\dot{x}_{ri}(t_+) = -e\,\dot{x}_{ri}(t_-), \tag{13a}$$
$$x_{ri}(t_+) = x_{ri}(t_-), \tag{13b}$$

where e is the restitution coefficient.

Turbulent flow through the equivalent orifice, i.e. a single orifice whose area is the sum of the areas of the actual orifices present on the piston, is expressed as

$$q_{or} = c_d^{or} A_{or}\sqrt{\frac{2}{\rho}|p_2 - p_1|}\,\mathrm{sign}(p_2 - p_1) \tag{14}$$

where A_{or} is the section of the equivalent orifice and c_d^{or} its associated outflow coefficient (Ref. [26]).

Finally, the force generated by the damper is

$$F = (p_2 - p_1)A - c_{21}\dot{x}_p, \tag{15}$$

where c_{21} is the friction coefficient between piston and tube.

The equation of motion of the by-pass valve writes

$$m_s\ddot{x}_s + c_s\dot{x}_s + k_s x_s = -F_{prs} + k_m I, \tag{16}$$

where x_s is the spool displacement, m_s, c_s and k_s are, respectively, the spool mass, damping and stiffness, while F_{prs} is the pre-load force, k_m the electric motor constant and I the current. The flow through the by-pass valve is computed as

$$q_{byp} = c_d^b A_{byp}(x_s)\sqrt{\frac{2}{\rho}|p_2 - p_1|}\,\mathrm{sign}(p_2 - p_1), \tag{17}$$

where c_d^b is the outflow coefficient, and A_{byp} the flow passing area which depends on the spool displacement as

$$A_{byp}(x_s) = \pi d_s x_s, \tag{18}$$

d_s being the spool diameter.

The coupled system of equations describing both the passive and the adaptive hydraulic damper configurations are stiff because of the high values of the oil bulk modulus, and because of the valve unilateral conditions which cause contact-impact events. Their integration in time was performed using a time-step-adaptive modified Rosenbrock formula of order 2 (see Ref. [27]).

REFERENCES

[1] Reed, D.A., "Lag Frequency Selective Damper," US Patent No. 3,638,885, Feb. 1, 1972.

[2] Anusonti-Intra, P., Gandhi, F., and Miller, L., "Reduction of Helicopter Vibration through Cyclic Control of Variable Orifice Dampers," *The Aeronautical Journal*, Vol. 107, 2003, pp. 657–672.

[3] Titurus, B., and Lieven, N., "Modeling and Analysis of Semi-Active Dampers in Periodic Working Environments," *AIAA Journal*, Vol. 47, No. 10, 2009, pp. 2404–2416.

[4] Titurus, B., and Lieven, N., "Integration of Hydraulic Lag-Damper Models with Helicopter Rotor Simulations," *Journal of Guidance, Control, and Dynamics*, Vol. 33, No. 1, 2010, pp. 200–211.

[5] Zhao, Y., Choi, Y.-T., and Wereley, N.M., "Semi-Active Damping of Ground Resonance in Helicopters using Magnetorheological Dampers," *Journal of the American Helicopter Society*, Vol. 49, 2004, pp. 468–483.

[6] Hu, W., Wereley, N.M., and Chen, P.C., "Semi-Active Linear Stroke Magnetorheological Fluid-Elastic Helicopter Lag Damper," *Journal of Guidance, Control, and Dynamics*, Vol. 30, No. 2, 2010, pp. 565–575.

[7] Bauchau, O.A., Van Weddingen, Y., and Agarwal, S., "Semiactive Coulomb Friction Lead-Lag Dampers," *Journal of the American Helicopter Society*, Vol. 55, 2010, pp. 012005-1–12.

[8] Bauchau, O.A., Bottasso, C.L., and Nikishkov, Y.G., "Modeling Rotorcraft Dynamics with Finite Element Multibody Procedures," *Mathematics and Computer Modeling*, Vol. 33, 2001, pp. 1113–1137.

[9] Bauchau, O.A., and Liu, H., "On the Modeling of Hydraulic Components in Rotorcraft Systems," *Journal of the American Helicopter Society*, Vol. 51, 2006, pp. 175–184.

[10] Johnson, W., "Self-Tuning Regulators for Multicyclic Control of Helicopter Vibration," NASA Technical Paper TP 1996, March 1982.

[11] Nguyen, K., Betzina, M., and Kitaplioglu, C., "Full-Scale Demonstration of Higher Harmonic Control for Noise and Vibration Reduction on the XV-15 Rotor," Army/NASA Rotorcraft Division, NASA Ames Research Center, Moffett Field, CA, 2000.

[12] Lovera, M., Colaneri, P., Malpica, C., and Celi, R., "Discrete-Time, Closed-Loop Aeromechanical Stability Analysis of Helicopters with Higher Harmonic Control", *Journal of Guidance, Control and Dynamics*, Vol. 30, 2007, pp. 1249–1260.

[13] Parks, T.W., and Burrus, C.S., *Digital Filter Design*, John Wiley & Sons, 1987.

[14] Hauer, J.F., Demeure, C.J., and Scharf, L.L., "Initial Results in Prony Analysis of Power System Response Signals," *IEEE Transaction on Power System*, Vol. 5, No. 1, 1990, pp. 80–89.

[15] Trudnowski, D.J., Johnson, J.M., and Hauer, J.F., "Making Prony Analysis More Accurate using Multiple Signals," *IEEE Transaction on Power System*, Vol. 14, 1999, pp. 226–231.

[16] Bottasso, C.L., Croce, A., Cacciola, S., and Gupta, S., "Estimation of Damping for Wind Turbines Operating in Closed-Loop," EWEC 2010, European Wind Energy Conference & Exhibition, Warsaw, Poland, April 20–23, 2010.

[17] Ljung, L., *System Identification — Theory for the User*, Prentice Hall, 1999.

[18] Johnson, W., *Helicopter Theory*, Princeton University Press, Princeton, NJ, 1981.

[19] Bittanti, S., and Colaneri, P., "Invariant Representations of Discrete-Time Periodic Systems," *Automatica*, Vol. 36, 2000, pp. 1777–1793.

[20] Duym, S.W.R., Stiens, R., and Reybrouck, K., "Evaluation of Shock Absorber Models," *Vehicle System Dynamics*, Vol. 27, No. 2, 1997, pp. 109–127.

[21] Duym, S.W.R., "Simulation Tools, Modeling and Identification, for an Automotive Shock Absorber in the Context of Vehicle Dynamics," *Vehicle System Dynamics*, Vol. 33, No. 4, 2000, pp. 261–285.

[22] Eyres, R.D., Champneys, A.R., and Lieven, N.A.J., "Modeling and Dynamic Response of a Damper with Relief Valve," *Nonlinear Dynamics*, Vol. 40, 2005, pp. 119–147.

[23] Eyres, R.D., Piiroinen, P.T., Champneys, A.R., and Lieven, N.A.J., "Grazing Bifurcation and Chaos in the Dynamics of a Hydraulic Damper with Relief Valves," *SIAM Journal of Applied Dynamical Systems*, Vol. 4, No. 4, 2005, pp. 1076–1106.

[24] Hayashi, S., Hayase, T., and Kurahashi, T., "Chaos in Hydraulic Control Valve," *Journal of Fluids and Structures*, Vol. 11, 1997, pp. 693–716.

[25] Habing, R.A., and Peters, M.C.A.M., "An Experimental Method for Validated Compressor Valve Vibration Theory," *Journal of Fluids and Structures*, Vol. 22, 2006, pp. 683–697.

[26] Ramamurthi, K., and Nandakumar, K., "Characteristics of Flow Through Small Sharp-Edged Cylindrical Orifices," *Flow Measurement and Instrumentation*, Vol. 10, 1999, pp. 133–143.

[27] `Matlab`, The MathWorks Inc., 3 Apple Hill Drive, Natick, MA 01760-2098, USA, `www.mathworks.com`.